JOURNAL OF Materials CHEMISTRY

Formation and catalytic characterization of various rare earth phosphates

Hiroaki Onoda,[a] Hiroyuki Nariai,*[a] Ai Moriwaki,[b] Hideshi Maki[b] and Itaru Motooka[b]

[a]*Department of Molecular Science, Graduate School of Science and Technology, Kobe University, 1-1, Rokkodai-cho, Nada-ku, Kobe 657-8501, Japan. E-mail: nariai@cx.kobe-u.ac.jp*
[b]*Department of Chemical Science and Engineering, Faculty of Engineering, Kobe University, 1-1, Rokkodai-cho, Nada-ku, Kobe 657-8501, Japan*

Received 6th November 2001, Accepted 11th April 2002
First published as an Advance Article on the web 29th April 2002

Various rare earth phosphates [rare earth elements: R = La, Ce, Pr, Nd, Sm, Yb, and Y; phosphates: Monazite-type, Xenotime-type, Rhabdophane-type, and Weinshenkite-type orthophosphates RPO_4, polyphosphate $R(PO_3)_3$, and ultraphosphate RP_5O_{14}] were synthesized by heating the mixtures of each rare earth oxide and diammonium hydrogenphosphate or phosphoric acid. The compositions of rare earth phosphates were determined by XRD, FT-IR, and TG–DTA. Catalytic properties were studied as one of properties of various rare earth phosphates. Specific surface areas of samples were measured by the BET method. Acid strengths and amounts of acidic sites were measured using several indicators by n-butylamine titration. Acidic properties were also confirmed by adsorption of ammonia. Various rare earth phosphates were characterized by catalytic activities on dehydration reaction of 2-propanol, cracking/dehydrogenation reaction of cumene, and isomerization reaction of butene. The characterization of catalysts was discussed with regard to type of rare earth elements, type of phosphates, and type of phosphorus resources.

Introduction

Phosphates transform to various other phosphates with hydrolysis and dehydration reactions by heating.[1,2] Phosphates have been used for ceramic materials, catalysts, fluorescent materials, dielectric substances, fuel cells, *etc*.[3–12] There are, however, fewer studies about rare earth phosphates than other metal phosphates. Anhydrous rare earth orthophosphate is the main component of natural Monazite and Xenotime which are rare earth element ores. Rhabdophane-type rare earth orthophosphates have a specific structure with vacant spaces.[13] Polyphosphates have chain structures in which tetrahedral PO_4 groups are linked together by oxygen bridges.[14] Rare earth ultraphosphates have a network structure which includes the anion represented by $P_5O_{14}^{3-}$.[15] A large proportion of ultraphosphates are not stable for hydrolysis reaction. However, rare earth ultraphosphate is stable.

The transformation of aliphatic primary and secondary alcohols to olefins and/or carbonyl compounds on acidic and basic catalysts has been studied.[16–20] The dehydration occurs on acidic sites, whereas the dehydrogenation is preferred in the presence of basic or redox sites. Both dehydration and dehydrogenation reactions of 2-propanol occur on the acid and basic sites, respectively. Therefore, these reactions are used as proof of acidic or basic catalysts.[3–9] 2-Propanol transforms to propylene on acidic catalysts and to acetone on basic catalysts. The conversion of 2-propanol to propylene is reported to be related to the amount of acidic sites.[3,5,9,10]

On the other hand, the cracking/dehydrogenation reaction of cumene is used to estimate Lewis and Brönsted acid sites of a catalyst from the product.[9,10,21] Cumene conversion gives cracking products as well as dehydrogenation products on acidic catalysts. Benzene and propylene are the cracking products mainly on Brönsted acid sites, whereas α-methylstyrene is a dehydrogenation product chiefly on Lewis acid sites.

The migration reaction of the double bond and the *cis–trans* isomerization reaction in olefin molecules occurs over many materials fields. Butene has the minimum number of carbon atoms for an olefin compound in which both reactions could take place. Hence, the isomerization reaction of n-butene is used as a representation of an isomerization reaction of an olefin.[22–25]

In this work, various rare earth phosphates (rare earth elements: R = La, Ce, Pr, Nd, Sm, Yb, and Y; phosphates: Monazite-type, Xenotime-type, Rhabdophane-type, and Weinshenkite-type orthophosphates, polyphosphate, and ultraphosphate) were investigated with regard to their catalytic aspects.

Experimental

Preparation of various rare earth phosphates

Various rare earth phosphates (rare earth elements: R = La, Ce, Pr, Nd, Sm, Yb, and Y; phosphates: Monazite-type, Xenotime-type, Rhabdophane-type, and Weinshenkite-type orthophosphates, polyphosphate, and ultraphosphate) were prepared by heating the mixtures of rare earth oxide and $(NH_4)_2HPO_4$ or H_3PO_4 in the ratios of phosphorus and rare earth elements $P:R$ = 1, 2, 3, 4, and 10. Thermal products were analyzed by X-ray diffractometry (XRD), Fourier transform infrared spectroscopy (FT-IR), and thermogravimetry–differential thermal analyses (TG–DTA). X-Ray diffraction patterns were recorded on a Rigaku Denki RINT 1200 M X-Ray diffractometer, using monochromated Cu $K\alpha_1$ radiation (λ = 0.154 nm). The IR spectra were recorded on a HORIBA FT-IR spectrometer FT-710 with a KBr disk method. TG–DTA were carried out at a heating rate of 10 °C min^{-1}, using a Rigaku Denki Thermo Plus TG8120

Estimation of surface properties

The surface areas of materials were calculated from the amount of nitrogen gas adsorbed at the temperature of liquid nitrogen by a five-point BET method (P/P_0 = 0.10, 0.15, 0.20, 0.25 and 0.30) with a Gemini-Micromeritics 2360 from Shimadzu Corp. Ltd. Acidic properties (acidic strength and amount of acidic

 DOI: 10.1039/b110121h

sites) were examined *via* n-butylamine titration using Hammett indicators because the pK_a of an indicator is the factor which determines the level of the acid strength of the titrated acid sites. The Hammett indicators were methyl red (pK_a = +4.8), dimethyl yellow (pK_a = +3.3), benzeneazodiphenylamine (pK_a = +1.5), and dicinnamalacetone (pK_a = −3.0). Acidic properties were also confirmed by adsorption of ammonia. 0.1 g of a rare earth phosphate was heated at 150 °C for 2 h under nitrogen gas, cooled to room temperature, and then placed in 3 litres of 1040 ppm ammonia gas-balanced nitrogen gas for 24 h. Then this phosphate was also analyzed by XRD, FT-IR and TG–DTA.

Dehydration reaction of 2-propanol

The conversion was calculated using the dehydration reaction of 2-propanol on a gas chromatograph G-3000 from Hitachi Corp. Ltd. A column (i.d. 3 mm and length 2 m) packed with Porapak Q and a thermocoupled detector were used. Helium was used as carrier gas at a flow rate of 20 mL min^{-1}. The pulse volume of 2-propanol was 0.8 μL. Injected 2-propanol was vaporized and carried to the catalyst phase. 2-Propanol and catalytic products – propylene and water – were separated in the column and detected.

0.2 g of a rare earth phosphate was mixed with *ca.* 2 mg of glass wool and then packed in a glass tube with *ca.* 10 mg of glass wool at both ends. Beforehand, the glass wool was confirmed to have no activity in this reaction.

Cracking/dehydrogenation reaction of cumene

The conversion was calculated using the cracking/dehydrogenation reaction of cumene on a gas chromatograph G-3900 from Hitachi Corp. Ltd. A column (i.d. 3 mm and length 2 m) packed with 15% TCEP on Uniport B (GL Science) and a thermocouple detector were used. Helium was used as carrier gas at a 20 mL min^{-1} flow rate. The pulse volume of cumene was 0.5 μL. Other conditions were the same as for the system for dehydration of 2-propanol.

Isomerization reaction of butene

Catalytic reaction was carried out in a closed gas circulation system.[26] 0.2 g of phosphate was packed into the glass reaction tube, and then 1-butene (Tokyo Kasei) was introduced into the reaction system. The reaction gases were analyzed using a Yanaco G2800 gas chromatograph with a VZ-7 column, which was connected directly to the gas circulation system.

Results and discussion

Formation and surface properties

Monazite-type rare earth (La, Ce, Pr, Nd, and Sm) orthophosphates and Xenotime-type rare earth (Yb and Y) orthophosphates were formed by heating the mixture of $P:R = 1$ at 1000 °C for 20 h from $(NH_4)_2HPO_4$, while Monazite-type rare earth (La, Ce, Pr, Nd, and Sm) orthophosphates and Xenotime-type rare earth (Yb and Y) orthophosphates were formed at 700 °C for 20 h from H_3PO_4. Rhabdophane-type rare earth (La, Pr, Nd, and Sm) orthophosphates were obtained by heating the mixture of $P:R = 1$ at 150 °C for 20 h from H_3PO_4. Weinschenkite-type rare earth (Y and Yb) orthophosphates were obtained by heating the mixture of $P:R = 1$ at 80 °C for 20 h from H_3PO_4. Rare earth (La, Ce, Pr, Nd, Sm, Yb, and Y) polyphosphates were prepared by heating the mixtures of $P:R = 3$ at 700 °C for 20 h. Lanthanum, cerium, praseodymium, neodymium, and samarium ultraphosphates were obtained by heating mixtures of $P:R = 10$ at 700 °C for 20 h and then washing with water to remove the excess phosphoric acid. These rare earth phosphates except for cerium salts were determined to be single phase materials from XRD analyses. The assignments of these XRD results were based on previous reports.[27,28]

Cerium salts of $P:Ce = 1$, 2, 3, and 4 were the mixtures of various cerium phosphates, Monazite-type $CePO_4$, CeP_2O_7, $Ce(PO_3)_3$, $Ce(PO_3)_4$, and CeP_5O_{14} by heating at 700 °C for 20 h. However, in this report, Monazite-type $CePO_4$, CeP_2O_7, $Ce(PO_3)_3$, and $Ce(PO_3)_4$ are defined as the samples prepared of $P:Ce = 1$, 2, 3, and 4, respectively.

Samples contained an amorphous phase which did not interfere with the experiments. It is difficult to obtain crystalline rare earth phosphates which do not have an amorphous phase. Therefore, in this work, the difference between crystalline and amorphous phase was not studied.

TG–DTA, XRD, and FT-IR results indicated that Rhabdophane-type rare earth (La, Pr, Nd, and Sm) orthophosphates lost their crystalline water at *ca.* 240 °C with their structure being maintained. However, Weinshenkite-type rare earth (Yb and Y) orthophosphates transformed to Xenotime-type rare earth orthophosphates at *ca.* 250 °C by loss of crystalline water.

Table 1 shows the specific surface areas of various rare earth phosphates. Specific surface areas of Monazite-type rare earth (La, Pr, Nd, and Sm) orthophosphates and Xenotime-type rare earth (Yb and Y) orthophosphates prepared from $(NH_4)_2HPO_4$ were smaller than 2 m^2 g^{-1}, whereas those prepared from H_3PO_4 were *ca.* 20–30 m^2 g^{-1}, except for the cerium salts. It was considered that the synthesis temperature had an influence on the specific surface areas. Because of the high synthesis temperature, these orthophosphates had small

Table 1 Specific surface areas of various rare earth phosphates[a] /m^2 g^{-1}

		La	Ce	Pr	Nd	Sm	Yb	Y
M-RPO_4	$(NH_4)_2HPO_4$	0.9	0.5	1.7	0.7	0.8	—[b]	—
	H_3PO_4	19.7	0.9	22.5	24.4	21.7	—	—
X-RPO_4	$(NH_4)_2HPO_4$	—	—	—	—	—	1.3	1.6
	H_3PO_4	—	—	—	—	—	20.7	29.2
R-RPO_4	H_3PO_4	85.0	—	57.7	86.5	75.6	—	—
W-RPO_4	H_3PO_4	—	—	—	—	—	16.8	17.8
RP_2O_7	$(NH_4)_2HPO_4$	—	0.8	—	—	—	—	—
	H_3PO_4	—	0.3	—	—	—	—	—
$R(PO_3)_3$	$(NH_4)_2HPO_4$	0.4	0.5	0.2	0.3	0.6	0.2	0.1
	H_3PO_4	2.1	0.5	0.1	0.2	0.4	0.1	0.2
$R(PO_3)_4$	$(NH_4)_2HPO_4$	—	0.1	—	—	—	—	—
	H_3PO_4	—	0.1	—	—	—	—	—
RP_5O_{14}	$(NH_4)_2HPO_4$	0.1	0.1	0.1	0.1	0.1	—	—
	H_3PO_4	0.2	0.3	0.3	0.2	0.2	—	—

[a]M-, X-, R- and W-RPO_4 represent Monazite-type, Xenotime-type, Rhabdophane-type, and Weinshenkite-type orthophosphates, respectively. [b]— Indicates that this phosphate was not formed.

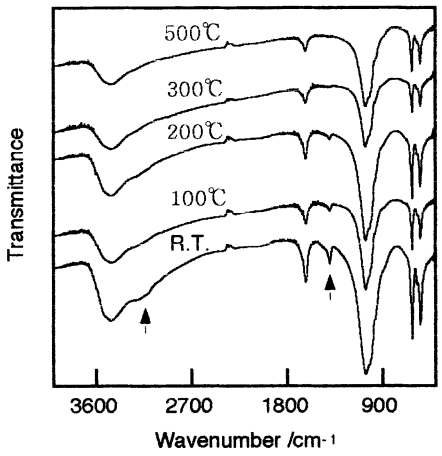

Fig. 1 IR spectra of Rhabdophane-type $NdPO_4$ adsorbed NH_3.

specific surface areas. Samples prepared at 1000 °C from H_3PO_4 had similar specific surface areas with those of samples synthesized from $(NH_4)_2HPO_4$. Monazite-type cerium orthophosphate had a small specific surface area, which differed from other Monazite-type rare earth (La, Pr, Nd, and Sm) orthophosphates. Rare earth (La, Ce, Pr, Nd, Sm, Yb, and Y) polyphosphates and rare earth (La, Ce, Pr, Nd, and Sm) ultraphosphates had smaller specific surface areas than each rare earth orthophosphate. Since the specific surface areas of these phosphates were very small, it is difficult to estimate catalytic activities based on specific surface areas. For this reason, the estimation of catalytic activity in this report was based on catalyst weight.

The n-butylamine titration using a Hammet indicator is easy and convenient for the estimation of acidic properties. Therefore, this method was used in this work. The acid strength of most rare earth phosphates was between -3.0 and $+1.5$ pK_a units. The amount of acidic sites at Ho $\leqslant +4.8$ was smaller than 3×10^{-4} mol g^{-1}. The acid strength and amount of acidic sites were influenced to only a small extent by the type of rare earth element, the type of various phosphates (orthophosphate, polyphosphate, and ultraphosphate), and the type of phosphorus resource [$(NH_4)_2HPO_4$ and H_3PO_4]. All rare earth phosphates that adsorbed ammonia had no change in TG–DTA and XRD results. However, new IR absorption peaks appeared by adsorbtion of ammonia in the case of rare earth phosphates which have a large specific surface area. Fig. 1 shows the IR spectra of Rhabdophane-type $NdPO_4$ which absorbed NH_3. The absorptions were observed at *ca.* 1400 and 3100 cm^{-1} which were considered to be due to NH_4^+. These absorptions disappered upon heating. This indicated that a certain amount of acid sites existed on surface of the material.

It was considered that catalytic activities of rare earth phosphates were influenced to a significant extent by specific surface area and only to a small extent by acidic properties.

Dehydration reaction of 2-propanol

Table 2 shows the conversion of 2-propanol to propylene over trivalent rare earth polyphosphates. Between 1.2 and 5.2% of 2-propanol transformed to propylene at 200 °C, 3.6–13.4% at 225 °C, and 12.2–32.1% at 250 °C. No unique rare earth polyphosphate was observed in this table. Acetone was not detected in this study. All rare earth phosphates had poor basic sites.

Table 3 shows the conversion of 2-propanol over various neodymium phosphates. Monazite-type and Rhabdophane-type neodymium orthophosphates prepared from H_3PO_4 had a higher catalytic activity than other neodymium phosphates. It was considered that the small specific surface area of Monazite-type neodymium orthophosphate prepared from $(NH_4)_2HPO_4$ caused its low activity. Neodymium polyphosphate and ultraphosphate had low activities for the dehydration reaction of 2-propanol.

Table 4 shows the conversion of 2-propanol over various cerium phosphates. Relatively, high conversion was obtained in the case of Monazite-type cerium orthophosphate prepared from H_3PO_4. Monazite-type cerium orthophosphate prepared from $(NH_4)_2HPO_4$ (900 °C, 20 h, specific surface area 0.15 m^2 g^{-1}) and cerium ultraphosphate prepared from $(NH_4)_2HPO_4$ indicated low conversion. The type of phosphate had less influence on catalytic activity in cerium phosphates than seen with other rare earth (La, Pr, Nd, Sm, Yb, and Y) phosphates.

Table 2 Conversion (%) of 2-propanol to propylene over rare earth polyphosphates

Rare earth element		Temperature/°C		
		200	225	250
La	$(NH_4)_2HPO_4$	3.9	10.5	32.1
Ce	$(NH_4)_2HPO_4$	3.5	8.7	23.2
Pr	$(NH_4)_2HPO_4$	1.6	4.3	14.0
Nd	$(NH_4)_2HPO_4$	2.3	5.6	13.9
Sm	$(NH_4)_2HPO_4$	4.0	9.3	26.7
Yb	$(NH_4)_2HPO_4$	1.2	3.9	12.2
Y	$(NH_4)_2HPO_4$	1.3	3.6	15.0
La	H_3PO_4	2.6	6.5	16.6
Ce	H_3PO_4	4.7	11.0	25.7
Pr	H_3PO_4	2.5	10.6	17.3
Nd	H_3PO_4	2.1	6.9	15.3
Sm	H_3PO_4	2.6	7.3	18.9
Yb	H_3PO_4	3.0	9.0	28.3
Y	H_3PO_4	5.2	13.4	21.6

Table 3 Conversion (%) of 2-propanol to propylene over neodymium phosphates[a]

Phosphate		Temperature/°C		
		200	225	250
M-$NdPO_4$	$(NH_4)_2HPO_4$[b]	0.2	1.0	1.0
	H_3PO_4	94.5	100.0	100.0
R-$NdPO_4$	H_3PO_4	100.0[c]	100.0	100.0
$Nd(PO_3)_3$	$(NH_4)_2HPO_4$	2.3	5.6	13.9
	H_3PO_4	2.1	6.9	15.3
NdP_5O_{14}	$(NH_4)_2HPO_4$	1.4	4.0	10.2
	H_3PO_4	0.9	1.6	5.2

[a]M- and R-$NdPO_4$ represent Monnzite-type and Rhabdophane-type $NdPO_4$, respectively. [b]This phosphate was prepared at 1000 °C for 20 h. [c]Extreme tailing was observed.

Table 4 Conversion (%) of 2-propanol to propylene over over cerium phosphates[a]

Phosphate		Temperature/°C		
		200	225	250
M-$CePO_4$	$(NH_4)_2HPO_4$[b]	0.7	0.8	1.7
	H_3PO_4	6.3	25.9	47.8
CeP_2O_7	$(NH_4)_2HPO_4$	3.8	10.9	28.6
	H_3PO_4	3.5	9.1	19.7
$Ce(PO_3)_3$	$(NH_4)_2HPO_4$	3.5	8.7	23.2
	H_3PO_4	4.7	11.0	25.7
$Ce(PO_3)_4$	$(NH_4)_2HPO_4$	2.7	7.5	18.3
	H_3PO_4	1.9	5.8	20.4
CeP_5O_{14}	$(NH_4)_2HPO_4$	1.3	3.6	8.6
	H_3PO_4	5.0	10.9	24.8

[a]M-$CePO_4$ represents Monazite-type $CePO_4$. [b]This phosphate was prepared at 900 °C for 20 h.

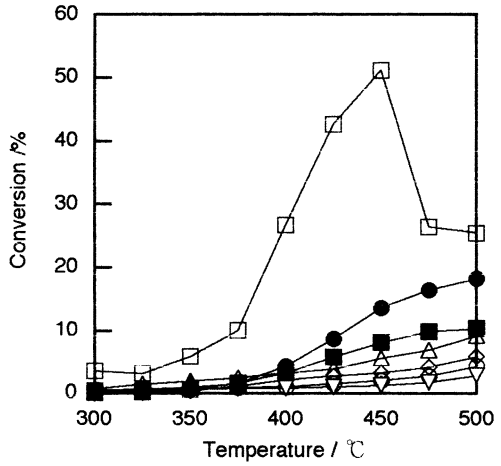

Fig. 2 Conversion of cumene over $R(PO_3)_3$ prepared from H_3PO_4: ○ La; □ Ce; ◇ Pr; △ Nd; ▽ Sm; ■ Yb; and ● Y.

Cracking/dehydrogenation reaction of cumene

Fig. 2 shows the conversion of cumene over rare earth polyphosphates prepared from H_3PO_4. The conversion over La, Pr, Nd, Sm, and Yb polyphosphates showed a monotonous increase with increasing temperature. The conversion over $Y(PO_3)_3$ increased slowly below 375 °C and more rapidly above 400 °C. Cerium polyphosphates had higher conversion than other rare earth (La, Pr, Nd, Sm, Yb, and Y) polyphosphates. Conversion over cerium polyphosphate had a maximum value at 450 °C. Fig. 3 shows the selectivity of cumene to benzene and propylene over these rare earth polyphosphates. A selectivity of 100% means that cumene transformed to benzene and propylene by cracking reaction; 0% selectivity means that cumene transformed to α-metylstylene by dehydrogenation reaction. Selectivity of cumene to benzene and propylene over rare earth polyphosphates generally increased with temperature. Lanthanum and samarium polyphosphates prepared from H_3PO_4 gave low selectivity of cumene to benzene and propylene. This indicated that these catalysts had poor Brönsted acid sites. Other rare earth (Ce, Pr, Nd, Yb, and Y) polyphosphates prepared from H_3PO_4 gave high selectivity of cumene to cracking products, benzene and propylene. There are rich Brönsted acid sites on these catalysts. Almost all phosphates had maximum selectivity at about 450 °C. Cerium polyphosphate had a large decrease of selectivity above this temperature. Furthermore, by calculating the yields of cracking products, the characteristic catalytic behavior of cerium phosphate became clear.

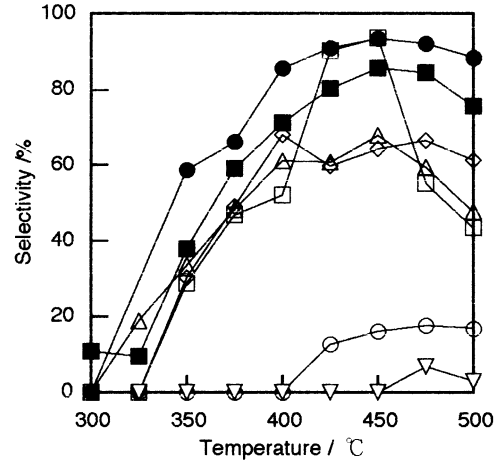

Fig. 3 Selectivity of cumene to benzene and propylene over $R(PO_3)_3$ prepared from H_3PO_4: ○ La; □ Ce; ◇ Pr; △ Nd; ▽ Sm; ■ Yb; and ● Y.

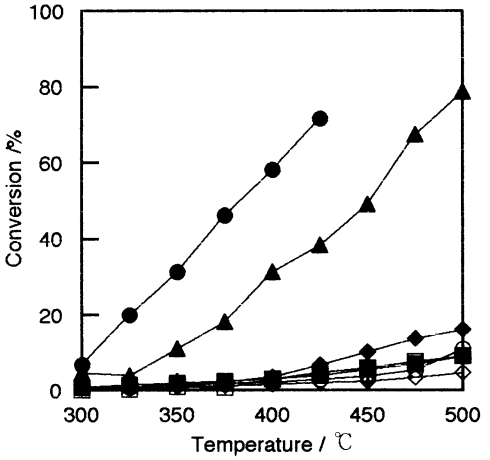

Fig. 4 Conversion of cumene over various neodymium phosphates: ○ Monazite-type $NdPO_4$ prepared from $(NH_4)_2HPO_4$; ● Monazite-type $NdPO_4$ prepared from H_3PO_4; ▲ Rhabdophane-type $NdPO_4$ prepared from H_3PO_4; □ $Nd(PO_3)_3$ prepared from $(NH_4)_2HPO_4$; ■ $Nd(PO_3)_3$ prepared from H_3PO_4; ◇ NdP_5O_{14} prepared from $(NH_4)_2HPO_4$; and ◆ NdP_5O_{14} prepared from H_3PO_4.

Fig. 4 shows the conversion of cumene over various neodymium phosphates. Monazite-type and Rhabdophane-type neodymium orthophosphates prepared from H_3PO_4 displayed high conversion of cumene and high selectivity to benzene and propylene. The retention time was long in the cases of Monazite-type and Rhabdophane-type neodymium orthophosphates prepared from H_3PO_4. Large specific surface areas of these phosphates were considered to lead to a long contact time by adsorption. A long contact time caused high conversion. At high temperature, the catalytic activity was not estimated due to tailing in the case of Monazite-type neodymium orthophosphate.

Monazite-type rare earth (La, Pr, Nd, and Sm) orthophosphates and Xenotime-type rare earth (Yb and Y) orthophosphates prepared from $(NH_4)_2HPO_4$ had low catalytic activity. Selectivity of cumene to benzene and propylene over Rhabdophane-type rare earth (La, Pr, Nd, and Sm) orthophosphates became smaller with increasing temperature. The selectivity over rare earth (La, Pr, Nd, and Sm) ultraphosphates was much affected by temperature.

Fig. 5 shows the conversion of cumene over various cerium phosphates prepared from H_3PO_4. Conversion of cumene over cerium phosphates increased with increasing temperature. CeP_2O_7 and $Ce(PO_3)_4$ gave maximum conversion at 425 °C.

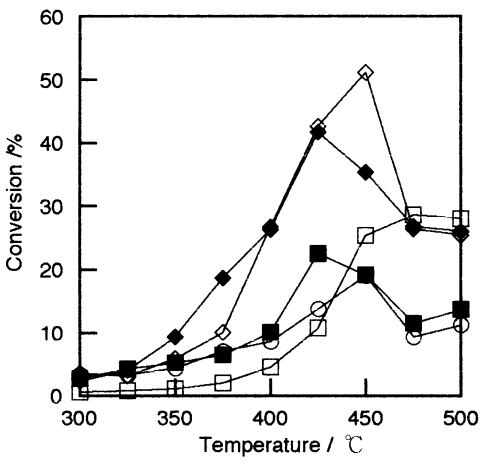

Fig. 5 Conversion of cumene over various cerium phosphates prepared from H_3PO_4: ○ Monazite-type $CePO_4$; ■ CeP_2O_7; ◇ $Ce(PO_3)_3$; ◆ $Ce(PO_3)_4$; and □ CeP_5O_{14}.

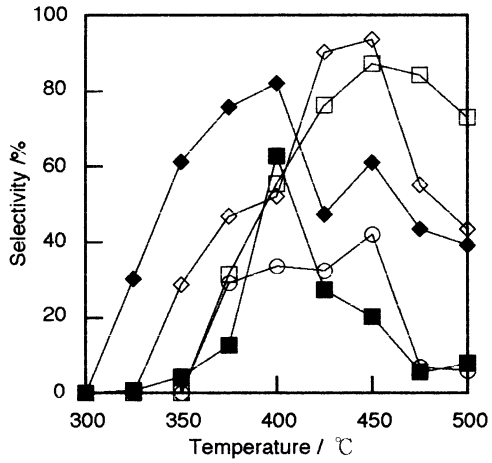

Fig. 6 Selectivity of cumene to benzene and propylene over various cerium phosphates prepared from H_3PO_4: ○ Monazite-type $CePO_4$; ■ CeP_2O_7; ◇ $Ce(PO_3)_3$; ◆ $Ce(PO_3)_4$; and □ CeP_5O_{14}.

Monazite-type $CePO_4$ and $Ce(PO_3)_3$ gave maximum conversions at 450 °C. Above 475 °C, a large decrease in conversion was observed except for CeP_5O_{14}. Fig. 6 shows the selectivity of cumene to benzene and propylene over these cerium phosphates prepared from H_3PO_4. The selectivity over CeP_2O_7 and $Ce(PO_3)_4$ had the maximum value at 400 °C. Monazite-type $CePO_4$ and $Ce(PO_3)_3$ had maximum selectivity at 450 °C. Monazite-type $CePO_4$ had lower catalytic activity than other Monazite-type rare earth (La, Pr, Nd, and Sm) orthophosphates. $Ce(PO_3)_3$ and $Ce(PO_3)_4$ had high activity. Cerium ultraphosphate indicated same tendency as with other rare earth (La, Pr, Nd, and Sm) ultraphosphates.

Figs. 7 and 8 show the XRD peak patterns of cerium phosphates prepared from H_3PO_4 before and after catalytic reaction, respectively. The sample in $P:Ce = 3$ before catalytic reaction is a mixture of $Ce(PO_3)_3$ and CeP_2O_7. The samples in $P:Ce = 10$ before and after catalytic reaction indicated the XRD peak pattern of CeP_5O_{14}. The peaks of CeP_2O_7 and $Ce(PO_3)_4$ became small in XRD results of samples after catalytic reaction. These results indicated that Ce(IV) phosphates were reduced to Ce(III) phosphates by use as a catalyst in the cracking/dehydrogenation reaction of cumene. Cerium phosphates were considered to be reduced by the following equations:

$$2\,CeP_2O_7 \rightarrow CePO_4 + Ce(PO_3)_3 + 1/2\,O_2$$

$$2\,Ce(PO_3)_4 \rightarrow Ce(PO_3)_3 + CeP_5O_{14} + 1/2\,O_2$$

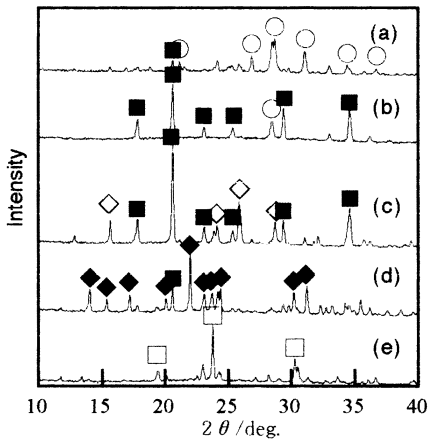

Fig. 7 XRD patterns of cerium phosphates prepared from H_3PO_4 before catalytic reaction: (a) $P:Ce = 1$; (b) $P:Ce = 2$; (c) $P:Ce = 3$; (d) $P:Ce = 4$; and (e) $P:Ce = 10$; ○ Monazite-type $CePO_4$; ■ CeP_2O_7; ◇ $Ce(PO_3)_3$; ◆ $Ce(PO_3)_4$; and □ CeP_5O_{14}.

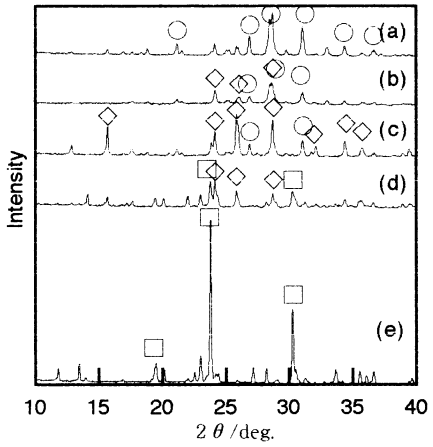

Fig. 8 XRD patterns of cerium phosphates prepared from H_3PO_4 after catalytic reaction: (a) $P:Ce = 1$; (b) $P:Ce = 2$; (c) $P:Ce = 3$; (d) $P:Ce = 4$; and (e) $P:Ce = 10$; ○ Monazite-type $CePO_4$; ◇ $Ce(PO_3)_3$; and □ CeP_5O_{14}.

The oxygen produced from these reactions attacked cumene in oxidative dehydrogenation. Cerium phosphates were reduced at *ca.* 400–425 °C and cumene was oxidised to α-methylstylene by the oxidative dehydrogenation reaction. XRD analyses indicated that all cerium phosphates were unchanged by heating under air conditions below 700 °C. These reactions caused low selectivity of cumene to benzene and propylene. Conversion of cumene over cerium phosphates became small by transformation from Ce(IV) phosphates to Ce(III) salts. It was considered that Ce(IV) phosphates had a higher catalytic activity than Ce(III) salts.

The oxidative dehydrogenation reaction of cumene to α-methylstylene was thought to cause the reduction of cerium phosphate. It was interesting that cerium phosphate reduced at *ca.* 400–450 °C in the presence of cumene.

Isomerization reaction of butene

Fig. 9 shows the conversion of 1-butene, selectivities to *cis*-2-butene and *trans*-2-butene, and the ratio of *cis*:*trans*-2-butene at several temperatures over Monazite-type $NdPO_4$ prepared from H_3PO_4 and Nd_2O_3. Conversion of 1-butene increased with increasing temperature; however, the ratio of *cis*:*trans*-2-butene decreased. Because *trans*-2-butene was more thermodynamically stable than *cis*-2-butene, 1-butene was considered

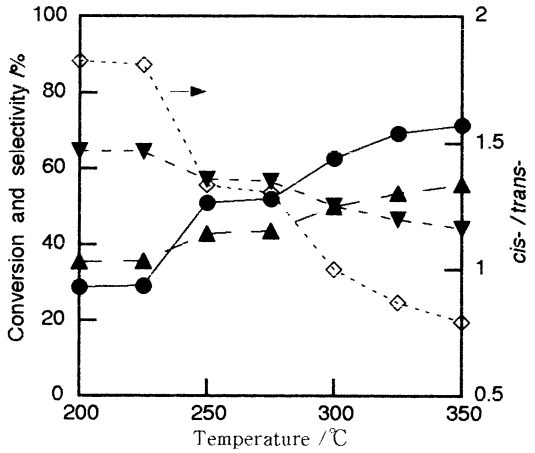

Fig. 9 Conversion of 1-butene (●), selectivity to *cis*-2-butene (▼) and to *trans*-2-butene (▲), and the ratio of *cis*:*trans*-2-butene (◇) at several temperatures over Monazite-type $NdPO_4$ prepared from H_3PO_4 (15.8 mg ml^{-1}, 200 torr).

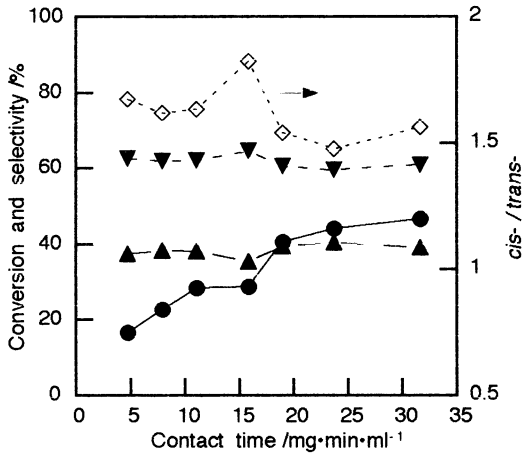

Fig. 10 Conversion of 1-butene (●), selectivity to *cis*-2-butene (▼) and to *trans*-2-butene (▲), and the ratio of *cis* : *trans*-2-butene (◇) over Monazite-type $NdPO_4$ prepared from H_3PO_4 at several contact times (200 °C, 200 torr).

to transform to *trans*-2-butene selectively at higher temperature. Fig. 10 shows the results of the isomerization reaction of butene over the above Monazite-type $NdPO_4$ for several contact times. In the case of BPO_4 (not shown), conversion of 1-butene was reported to have little change on contact time.[16] However, conversion of 1-butene over Monazite-type $NdPO_4$ increased with increasing contact time. The ratio of *cis* : *trans*-2-butene was less influenced by contact time. Fig. 11 shows the results of the isomerization reaction of butene over the Monazite-type $NdPO_4$ at several butene pressures. By an increase in the amount of the induced 1-butene molecule, conversion of 1-butene decreased a little. The ratio of *cis* : *trans*-2-butene was less changed by the initial amount of butene.

Table 5 shows the results of the isomerization reaction of butene over Monazite-type rare earth (La, Ce, Pr, Nd, and Sm) orthophosphates and Xenotime-type rare earth (Yb and Y) orthophosphates prepared from H_3PO_4. Cerium orthophosphate indicated lower conversion of 1-butene than other rare earth (La, Pr, Nd, Sm, Yb, and Y) orthophosphates. Table 6 shows the results over various neodymium phosphates. Monazite-type and Rhabdophane-type neodymium orthophosphates prepared from H_3PO_4 had high conversion of 1-butene. Neodymium polyphosphates and ultraphosphates prepared from $(NH_4)_2HPO_4$ and H_3PO_4 produced *cis*-2-butene selectively. Table 7 shows the results over various cerium phosphates. As mentioned above, cerium orthophosphate had a

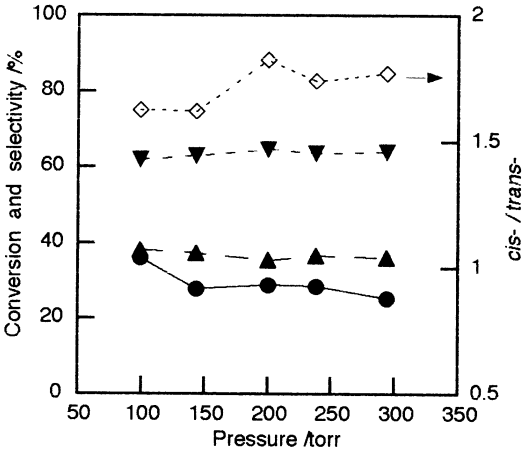

Fig. 11 Conversion of 1-butene (●), selectivities to *cis*-2-butene (▼) and to *trans*-2-butene (▲), and the ratio of *cis* : *trans*-2-butene (◇) over Monazite-type $NdPO_4$ prepared from H_3PO_4 at several butene pressures (200 °C, 15.8 mg min^{-1} ml^{-1}).

Table 5 Results of the isomerization reaction of butene over Monazite-type rare earth (La, Ce, Pr, Nd, and Sm) orthophosphates and Xenotime-type rare earth (Yb and Y) orthophosphates prepared from H_3PO_4 (300 °C, 15.8 mg min^{-1} ml^{-1}, 200 torr)

Rare earth element	Conversion (%)	Selectivity (%)		
		cis[a]	*trans*[a]	*cis* : *trans*
La	66.9	45.9	54.1	0.849
Ce	21.5	50.0	50.0	1.000
Pr	59.0	43.5	56.5	0.771
Nd	62.7	50.0	50.0	1.000
Sm	73.5	41.5	58.5	0.709
Yb	74.1	40.7	59.3	0.687
Y	77.8	40.6	59.4	0.685

[a]*cis* = *cis*-2-Butene, *trans* = *trans*-2-butene.

Table 6 Results of the isomerization reaction of butene over various neodymium phosphates[a] (300 °C, 15.8 mg min^{-1} ml^{-1}, 200 torr)

Phosphate		Conversion (%)	Selectivity (%)		
			cis[b]	*trans*[b]	*cis* : *trans*
M-$NdPO_4$	$(NH_4)_2HPO_4$[c]	6.5	46.5	53.6	0.867
	H_3PO_4	62.7	50.0	50.0	1.000
R-$NdPO_4$	H_3PO_4	62.5	46.5	53.5	0.868
$Nd(PO_3)_3$	$(NH_4)_2HPO_4$	29.5	58.9	41.1	1.431
	H_3PO_4	8.7	61.9	38.1	1.624
NdP_5O_{14}	$(NH_4)_2HPO_4$	1.6	55.6	44.4	1.250
	H_3PO_4	11.5	69.2	30.8	2.250

[a]M- and R-$NdPO_4$ represent Monazite- and Rhabdophane-type $NdPO_4$. [b]*cis* = *cis*-2-Butene, *trans* = *trans*-2-butene. [c]This phosphate was prepared at 1000 °C for 20 h. Other phosphates were prepared at 700 °C for 20 h.

Table 7 Results of the isomerization reaction of butene over various cerium phosphates[a] (300 °C, 15.8 mg min^{-1} ml^{-1}, 200 torr)

Phosphate		Conversion (%)	Selectivity (%)		
			cis[b]	*trans*[b]	*cis* : *trans*
M-$CePO_4$	$(NH_4)_2HPO_4$[c]	0	—	—	—
	H_3PO_4[d]	21.5	50.0	50.0	1.000
CeP_2O_7	$(NH_4)_2HPO_4$	21.8	59.9	40.1	1.493
	H_3PO_4	1.8	58.1	41.9	1.384
$Ce(PO_3)_3$	$(NH_4)_2HPO_4$	24.0	50.5	49.5	1.021
	H_3PO_4	15.4	59.0	41.0	1.441
$Ce(PO_3)_4$	$(NH_4)_2HPO_4$	9.9	62.4	37.6	1.658
	H_3PO_4	13.4	60.7	39.3	1.542
CeP_5O_{14}	$(NH_4)_2HPO_4$	0	—	—	—
	H_3PO_4	1.1	59.0	41.0	1.441

[a]M-$CePO_4$ represents Monazite-type $CePO_4$. [b]*cis* = *cis*-2-Butene, *trans* = *trans*-2-butene. [c]This phosphate was prepared at 900 °C for 20 h. [d]This phosphate was prepared at 600 °C for 20 h. Other phosphates were prepared at 700 °C for 20 h.

lower conversion than other rare earth (La, Pr, Nd, Sm, Yb, and Y) phosphates. However, cerium condensed phosphates [CeP_2O_7, $Ce(PO_3)_3$, $Ce(PO_3)_4$, and CeP_5O_{14}] indicated similar conversions of 1-butene and ratios of *cis*-/*trans*-2-butene with other rare earth (La, Pr, Nd, Sm, Yb, and Y) polyphosphates and ultraphosphates. Cerium condensed phosphates [CeP_2O_7, $Ce(PO_3)_3$, $Ce(PO_3)_4$, and CeP_5O_{14}] prepared from H_3PO_4 had similar selectivities for 1-butene to *cis*- and *trans*-2-butene. The kind of phosphorus resource had some influence on the catalytic activities for the isomerization reaction of butene.

Conclusion

Various rare earth phosphates (rare earth elements: R = La, Ce, Pr, Nd, Sm, Yb, and Y; phosphate: Monazite-type,

Xenotime-type, Rhabdophane-type, and Weinshenkite-type orthophosphates, polyphosphates, and ultraphosphates) were obtained by heating mixtures of the rare earth oxide and $(NH_4)_2HPO_4$ or H_3PO_4 in several ratios of phosphorus and rare earth elements. Rare earth orthophosphates prepared from H_3PO_4 had larger specific surface areas than rare earth polyphosphates and ultraphosphates. All rare earth phosphates were acidic catalysts, not basic catalysts. Catalytic activities of rare earth phosphates varied depending on the type of rare earth elements (La, Ce, Pr, Nd, Sm, Yb, and Y), type of phosphates (Monazite-type, Xenotime-type, Rhabdophane-type, and Weinshenkite-type orthophosphates, polyphosphates, and ultraphosphates), and type of phosphorus resources [$(NH_4)_2HPO_4$ and H_3PO_4]. In particular, cerium phosphates had characteristic catalytic activities.

References

1 M. Tsuhako, S. Ikeuchi, T. Matsuo, I. Motooka and M. Kobayashi, *Bull. Chem. Soc. Jpn.*, 1979, **52**, 1034.
2 A. F. Selevich, A. S. Lyakhov and A. I. Lesnikovich, *Phosphorus Res. Bull.*, 1999, **10**, 171.
3 H. Nariai, H. Taniguchi, H. Maki and I. Motooka, *Phosphorus Res. Bull.*, 1998, **8**, 119.
4 H. Onoda, H. Nariai, H. Maki and I. Motooka, *Phosphorus Res. Bull.*, 1999, **9**, 69.
5 M. R. Mostafa and A. M. Youssef, *Mater. Lett.*, 1998, **34**, 405.
6 K. Yamamoto and Y. Abe, *J. Am. Ceram. Soc.*, 1998, **81**, 2201.
7 E. A. El-Sharkawy, M. R. Mostagfa and A. M. Youssef, *Colloids Surf., A*, 1999, **157**, 211.
8 J. J. Jimenez, P. M. Maireles, A. J. Lopez and E. R. Castellon, *J. Solid State Chem.*, 1999, **147**, 664.
9 T. Mishra, K. M. Parida and S. B. Rao, *Appl. Catal. A*, 1998, **166**, 115.
10 A. C. B. dos Santos, W. B. Kover and A. C. Faro, *Appl. Catal. A*, 1997, **153**, 83.
11 Y. Takita, K. Sano, T. Muroya, H. Nishiguchi, N. Kawata, M. Ito, T. Akbay and T. Ishihara, *Appl. Catal. A*, 1998, **170**, 23.
12 Y. Takita, M. Ninomiya, H. Miyake, H. Wakamatsu, Y. Yoshinaga and T. Ishihara, *Phys. Chem. Chem. Phys.*, 1999, **1**, 4501.
13 R. C. L. Mooney, *Acta Crystallogr.*, 1950, **3**, 337.
14 H. Y.-P. Hong, *Acta Crystallogr., Sect. B*, 1974, **30**, 468.
15 D. Stachel and A. Olbertz, *Phosphorus Res. Bull.*, 1999, **10**, 70.
16 J. B. Moffat, *Catal. Rev. Sci. Eng.*, 1978, **18**, 199.
17 Y. Sakai and H. Hattori, *J. Catal.*, 1976, **42**, 37.
18 R. F. Vogel and G. Marcelin, *J. Catal.*, 1983, **80**, 492.
19 A. Schmidmeyer and J. B. Moffat, *J. Catal.*, 1985, **96**, 242.
20 H. Itoh, A. Tada, H. Hattori and K. Tanabe, *J. Catal.*, 1989, **115**, 244.
21 M. A. Aramendia, V. Borau, C. Jimenez, J. M. Marinas, F. J. Romero and J. R. Ruiz, *J. Colloid Interface Sci.*, 1998, **202**, 456.
22 A. Waghray and E. I. Ko, *Catal. Today*, 1996, **28**, 41.
23 S. Gao and J. B. Moffat, *J. Catal.*, 1998, **180**, 142.
24 R. A. Boyse and E. I. Ko, *Catal. Lett.*, 1996, **38**, 225.
25 P. Meriaudeau, A. V. Tuan, N. L. Hung and G. Szabo, *Catal. Lett.*, 1997, **47**, 71.
26 K. Nakamura, K. Eda, S. Hasegawa and N. Sotani, *Appl. Catal. A*, 1999, **178**, 167.
27 A. Durif, *Crystal Chemistry of Condensed Phosphates*, Plenum Publishing Corp., New York, 1995.
28 M. T. Averbuch-Pouchot and A. Durif, *Topics in Phosphate Chemistry*, World Scientific Publishing, Singapore, 1996.